



Zwitterionic poly(terphenylene piperidinium) membranes for vanadium redox flow batteries

Ivan Salmeron-Sanchez^{a,b}, Pegah Mansouri Bakvand^c, Anuja Shirole^c,
Juan Ramón Avilés-Moreno^b, Pilar Ocón^b, Patric Jannasch^c, Rakel Wreland Lindström^a,
Amirreza Khataee^{a,*}

^a Division of Applied Electrochemistry, Department of Chemical Engineering, KTH Royal Institute of Technology, SE-100 44 Stockholm, Sweden

^b Universidad Autónoma de Madrid (UAM), Departamento de Química Física Aplicada, C/Francisco Tomás y Valiente 7, 28049 Madrid, Spain

^c Department of Chemistry, Lund University, P.O. Box 124, SE-221 00 Lund, Sweden

ABSTRACT

Over recent years, non-fluorinated ion exchange membranes based on poly(terphenylene) backbones carrying different functional groups have shown potential application for vanadium redox flow batteries (VRFBs). Generally, the ion exchange membrane in VRFBs is a critical component in terms of the output power, long-term stability and cost. Yet, the shortcomings of commercial membranes (e.g., Nafion) have become a substantial barrier to further commercializing VRFBs. After successfully fabricating and testing poly(terphenylene)-based membranes carrying piperidinium and sulfonic acid groups, respectively, for VRFBs, we have in the present work combined both these ionic groups in a single zwitterionic membrane. A series of poly(terphenylene)-based membranes containing zwitterionic (sulfonated piperidinium) and cationic (piperidinium) groups in different ratios (40–60%) were synthesized and investigated. The VRFB using the zwitterionic membranes showed competitive performance compared to Nafion 212 regarding ionic conductivity, capacity retention, and chemical stability. In addition, it was shown that the VRFB performance was improved by increasing the content of zwitterionic groups within the membrane. A self-discharge time of more than 800 h and 78.7% average capacity retention for 500 VRFB cycles were achieved using a membrane with an optimized ratio (60% zwitterionic and 40% piperidinium groups). Furthermore, the chemical stability was promising, as there was no change in the chemical structure after 500 cycles. Our results represent a critical step for developing novel and competitive ion exchange membranes as an excellent alternative to the Nafion benchmark.

1. Introduction

The exploitation of eco-friendly and renewable energy sources (e.g., solar and wind) must be coupled with large-scale energy storage systems to satisfy the demand for reliable energy and holding power supply [1,2]. In this context, vanadium redox flow batteries (VRFBs) have come into focus due to their excellent flexibility in design and operation (decoupled power and energy), long-life span, moderate operating conditions, low maintenance costs, and tolerance to deep discharge and overcharge [3–6]. VRFBs are suitable for medium-to-large scale (kWh to MWh) energy storage applications with excellent cyclability and high energy efficiency [7–10]. Moreover, VRFBs use the same element in both half-cells, which means that capacity decay can be restored by rebalancing the electrolytes [11–13].

Broad commercialization of VRFBs is still hampered by both high cost and the fluorinated structure or, more importantly, unsatisfactory performance (insufficient chemical stability and poor ion selectivity) of commercially available membranes [14,15]. For instance, the most

widely used membrane, Nafion, is chemically robust and very conductive in acidic media; however, Nafion firstly belongs to the group of per- and polyfluoroalkyl substances (PFASs) and secondly suffers from poor ion-selectivity causing severe vanadium ion crossover and capacity fade [14]. Therefore, a sustainable membrane that fulfills an excellent balance between performance features is critically essential for the successful implementation of VRFBs.

One possible but still not perfect approach is the exploration of chemical and/or physical modifications of Nafion membranes (e.g., the incorporation of a graft polymer via radiation-induced polymerization, the incorporation of inorganic nanoparticles, etc.) to reduce the electrolyte crossover while maintaining the identical or higher conductivity and water uptake compared to Nafion. Successful cases could be a combination of Nafion with polytetrafluoroethylene, silica, titanium oxide, and graphene oxide [16–21]. Furthermore, the modified Nafion membranes are evidently as chemically stable as Nafion, but the challenging process is to balance the permeability of vanadium and the conductivity of the membrane. Another main challenge is that the

* Corresponding author.

E-mail address: khat@kth.se (A. Khataee).

<https://doi.org/10.1016/j.cej.2023.145879>

Received 16 July 2023; Received in revised form 17 August 2023; Accepted 3 September 2023

Available online 4 September 2023

1385-8947/© 2023 The Author(s). Published by Elsevier B.V. This is an open access article under the CC BY license (<http://creativecommons.org/licenses/by/4.0/>).

European Chemicals Agency will prohibit the use of PFASs through late 2030. For the latter, one can think about combining highly acidic and conductive sulfonic acid groups with non-fluorinated backbones. Some approaches in this direction have been followed by preparing and evaluating anion exchange membranes (AEMs) and cation exchange membranes (CEMs) based on hydrocarbon polymer backbones and various ion exchange groups [22–24]. Poly(arylene) structures without any fluorine content have recently shown competitive chemo-mechanical stability to Nafion due to the aromatic backbone. In addition, the presence of the arylene units in the polymer backbone allows for incorporating various functional groups, side chains, or modifications, enabling the fine-tuning of membrane properties. It should be noted that poly(arylene) structures containing ether bonds are not discussed here, as ether bonds may be susceptible to attack by vanadium (V) species. Yuan et al. [25] have reported on the degradation of polysulfone-based CEM through the formation of a phenolic hydroxyl group and vanadium(IV) oxygen species. Our previous study [26] on poly(arylene)-based CEMs is a good example where adding sulfonic acid groups on perfluoroalkyl- and perfluorophenyl side chains, respectively, resulted in comparable properties to Nafion. Higher water uptake and ion-exchange capacity (IEC) but lower vanadium permeability were measured for these membranes in comparison with Nafion. Moreover, using perfluorophenyl side chains, a higher ionic conductivity than Nafion was obtained. Poly(arylene) backbones can also be combined with positively charged functional groups to form anion exchange membranes (AEMs). Wang et al. [27] functionalized these backbones with pendant quaternary ammonium-tethered alkyl chains. Interesting results were achieved by varying the number of phenyl groups in the backbone. The biphenyl type had a higher water uptake and IEC while having higher vanadium permeability than the terphenyl types. In addition, despite the significantly higher water uptake and IEC of the biphenyl type than Nafion, lower ion conductivity was measured, which is likely due to the partial contribution of anions rather than only protons in ion exchanging. In our subsequent investigation [28], we studied the integration of piperidinium functional groups with poly(arylene) backbones. The membrane outperformed Nafion in terms of restricted vanadium permeability, even though the water uptake was higher and the ionic conductivity was lower. Considering the same poly(terphenylene) backbones, it is remarkable that the combination of piperidinium and trifluoroacetophenone in this study resulted in two orders of magnitudes lower permeability than pendant quaternary ammonium-tethered alkyl chains in Wang's study [27]. All the abovementioned membranes have shown excellent chemo-mechanical stability through oxidation stability tests in vanadium (V) solution or flow cell tests. Generally, it is not straightforward to correlate the notable features of membranes to a specific functional group or backbone. For instance, quaternary ammonium groups and alkyl chains with high pK_a values are less acidic and less prone to hydrolysis in acidic media; however, higher water uptake and ionic conductivity compared to Nafion can be achieved when integrated with backbones in membranes [27]. In fact, the combined effects of the backbone type, side chains, and functional groups would determine the membrane's features.

Guided by our recent findings, we were curious to study the effect of having two functional groups with different charges in a single membrane on properties like water uptake and, more critically, VRFB performance. Such a concept is based on zwitterionic groups and can be studied using different backbones. Zwitterionic membranes contain functional groups that can simultaneously act as both anionic and cationic sites. The key idea is to improve ion selectivity further while maintaining high conductivity. For instance, Nafion was modified with amino-SiO₂ nanoparticles to provide sulfonic acid and quaternary ammonium groups [29]. This case can be similar to a Nafion/SiO₂ membrane with a vanadium permeability in the range between 10⁻⁷ and 35 h self-discharge time when used in a VRFB system [20]. Similar vanadium permeability for the zwitterionic Nafion was achieved for the same thickness, but the self-discharge time was two times longer. More

important, the ionic conductivity of Nafion/SiO₂ and Nafion/amino/SiO₂ membranes was rather close to that of Nafion. A similar trend was observed when modifying a sulfonated poly(ether ether ketone) with quaternized poly(ether imide) groups [30]. Increasing the content of positively charged groups improved the ion selectivity and reduced the VRFB capacity loss, while the ionic conductivity remained as high as for the non-modified membrane. The counter example corresponds to amphoteric sulfonated poly(ether ether ketone) membrane carrying imidazolium-functionalized polysulfone [31], where increasing the content of imidazolium-functionalized polysulfone up to 20% helped reduce the vanadium permeability and the VRFB capacity loss. However, the ionic conductivity dropped 43% compared to the non-modified sulfonated poly(ether ether ketone). The zwitterionic materials presented in the current study demonstrate that the ion selectivity can be further improved in relation to the corresponding CEM. However, the ionic conductivity depends on the specific functional ion group that needs to be increased. In this study, a series of poly(terphenylene)-based zwitterionic membranes were synthesized. The membranes carry zwitterionic moieties comprised of piperidinium and sulfonic acid groups. A part of functional group, the piperidinium-type ring, is capable of potential strengths due to the Donnan exclusion effect and reducing the cross-mixing of vanadium species. For comparison a homopolymer without any zwitterionic unit (ZW-0%) was also synthesized. Furthermore, we have investigated the effect of the content ratio between zwitterionic and piperidinium groups on the membrane properties and VRFB performance.

2. Experimental section

2.1. Materials

The following chemicals were purchased from Sigma-Aldrich, and were used as received: *p*-terphenyl (≥99.5%), *N*-methyl-4-piperidone (Pip, ≥98%), 1,4-butane sultone (≥99%), trifluoroacetic acid (TFA, 99%), trifluoromethane sulfonic acid (TFSA, ≥99%), ethanol (EtOH, reagent grade), potassium carbonate (K₂CO₃, ≥99%), sodium bromide (NaBr, ≥99%), sodium hydroxide (NaOH, 99% pellets), dichloromethane (DCM, reagent grade), dimethyl sulfoxide (DMSO, reagent grade), diethyl ether (Et₂O, reagent grade), 2-propanol (IPA, reagent grade), acetonitrile (MeCN, reagent grade), DMSO-*d*₆ (99.96% D) and D₂O (99.9% D).

Vanadium(V) oxide (V₂O₅, 99.2%) and vanadyl sulfate hydrate (VOSO₄·3H₂O, 99.9%) were obtained from Thermo Fisher Scientific. A commercial 1.6 M mixture of V³⁺/V⁴⁺ electrolyte in 2 M H₂SO₄ was purchased from the GfE company (Gesellschaft für Elektrometallurgie mbH). Magnesium sulfate (MgSO₄, ≥99.5%) was provided by Sigma-Aldrich, and carbon papers (GDL, Sigracet 29 BC) and Nafion 212 (N212) membranes were purchased from FuelCellStore. All chemicals employed in the battery performance studies were used as received without further purification.

2.2. Synthesis of 1-methyl-1-sulfobutyl-piperidine-4-one monomer (zwPip)

The zwitterionic piperidinium monomer (zwPip) was prepared by reacting Pip with 1,4-butane sultone. In a 25 mL round bottom flask connected to a water condenser, *N*-methyl piperidone (2.17 mL, 1 equiv.) and 1,4-butane sultone (3.6 mL, 2 equiv.) was added to 10 mL MeCN. The reaction was left under stirring at 60 °C for 24 h under reflux. During the reaction, the product precipitated out, and after the reaction, the product was filtered off and washed with fresh MeCN several times to remove any unreacted starting materials. The product (zwPip) was obtained in the form of a white powder and was finally dried in a vacuum oven at 50 °C for 48 h before further reaction.

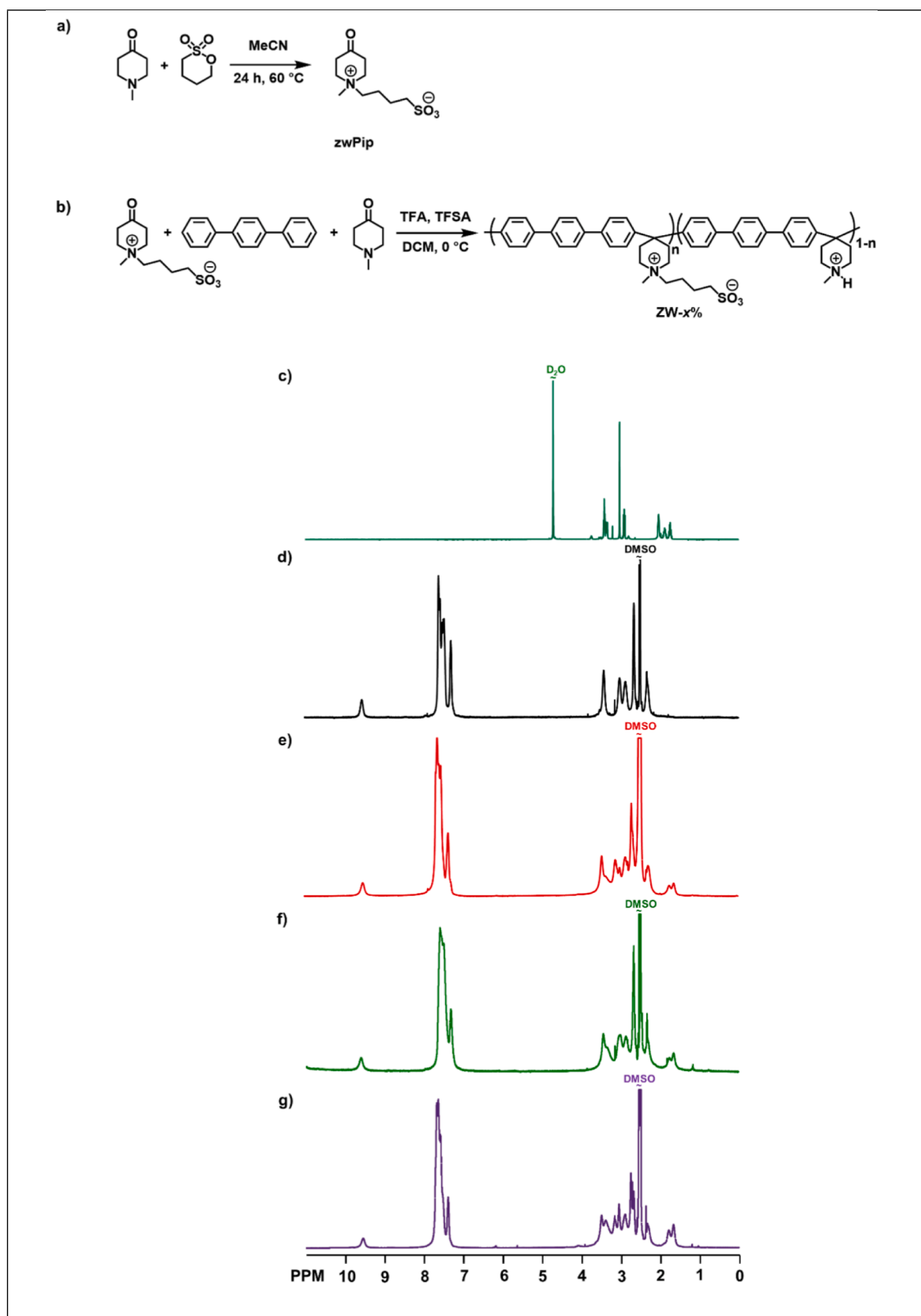


Fig. 1. Synthetic pathway to (a) monomer (zwPip) and (b) zwitterionic copolymers and ^1H NMR spectra of (c) zwPip, (d) ZW-0%, (e) ZW-40%, (f) ZW-50%, and (g) ZW-60%. The x% shows the content of zwitterionic groups versus piperidinium groups in the membrane.

2.3. Synthesis of poly(*p*-terphenylene piperidine)s containing zwitterionic groups (ZW-*x*%)

A series of zwitterionic poly(terphenylene piperidinium)s were prepared in superacid-mediated Friedel-Crafts type co-polycondensations of *p*-terphenyl and a mixture of Pip and zwPip at a controlled ratio. The samples were designated as ZW-*x*% where the *x* represents the percentage of zwitterionic content. Three copolymers, i.e., ZW-40%, ZW-50%, and ZW-60%, containing 37, 50, and 58 mol% zwitterionic groups, respectively, were synthesized. The preparation of ZW-40% is given as an illustrative example. In a two-necked round bottom flask under nitrogen, 3.4 mL of DCM, 1 g *p*-terphenyl (1 equiv.), 0.54 mL Pip (1.2 equiv.), and 0.43 g (0.4 equiv.) zwPip were added. Then the flask was placed in an ice bath to lower the temperature to 0 °C before the addition of 4.31 mL (12.5 equiv.) TFSA and 0.59 mL (2 equiv.) TFA. The reaction was kept under stirring at 0 °C until it became highly viscous after around 7 h. The reaction mixture was then precipitated in water: EtOH (4:1, v:v) mixture. The white fibrous precipitate was filtered off and washed with fresh water several times to remove all the residual monomers and acids before being dried at 50 °C under vacuum for 48 h. ZW-50% and ZW-60% were synthesized following the same procedure.

A homopolymer without any zwitterionic groups (ZW-0%) was synthesized by using a mixture of *p*-terphenyl (1 equiv.), Pip (1.2 equiv.), TFSA (10 equiv.) and TFA (2 equiv.) in a polycondensation at 0 °C for 5–6 h. The product was isolated as described above and then confirmed by ¹H NMR spectroscopy (see Fig. 1).

2.4. Membrane preparation

Membranes were cast from 5 wt% solutions of the copolymers in DMSO. The polymer solutions were passed through a Teflon syringe filter (Millex LS, 5 µm) and poured onto glass Petri dishes (Ø = 5 cm). The Petri dishes were placed in an explosion-proof ventilated casting oven at 80 °C for 48 h. After drying, the membranes were peeled from the Petri dishes after adding water. The membranes were washed carefully with deionized water and then kept in fresh deionized water before further characterization. The thickness of all the membranes was kept at around 50 µm in order to make them comparable to the N212 membrane.

2.5. Characterization of synthesized membranes

2.5.1. Chemical structure analysis

¹H NMR analyses were conducted with a Bruker DR X400 spectrometer at 400.13 MHz using DMSO-*d*₆ (δ = 2.50 ppm) as a solvent with 5–10% TFA added to shift the water peak downfield and reveal any protons from tertiary amines. The spectrum of zwPip was recorded in D₂O.

2.5.2. Electrolyte uptake (EU) and swelling ratio (SR)

The electrolyte uptake and swelling ratio of the membranes were measured in H₂SO₄ solutions. First, the samples were completely dried under vacuum at 50 °C and then weighted and measured (*m*_{dry}, and *X*_d, *Y*_d, *Z*_d). The samples were placed in 2.5 and 5 M aqueous H₂SO₄, respectively, for 4 days at room temperature, refreshing the solutions at least three times during this period. After removing the membranes from the solution, the surface of the membranes was quickly wiped dry and then immediately weighed and measured (*m*_{wet}, and *X*_w, *Y*_w, *Z*_w). Finally, the electrolyte uptake and swelling ratio for each concentration and sample were calculated by using the following equations:

$$EU(\%) = \frac{m_{wet} - m_{dry}}{m_{dry}} \cdot 100\% \quad (1)$$

$$SR(\%) = \frac{X_w Y_w Z_w - X_d Y_d Z_d}{X_d Y_d Z_d} \cdot 100\% \quad (2)$$

Before the measurement, N212 was treated in 1 M H₂SO₄ at 100 °C for 2 h, and then it was washed several times with distilled water to remove excess acid. Subsequently, the samples were kept in distilled water for 2 h at 100 °C. Then it was ready to be treated as above-mentioned to measure the electrolyte uptake and swelling ratio.

2.5.3. Permeability of VO²⁺

The vanadium permeability through the membranes was measured by placing the membrane in a diffusional cell (H-type) with an active area of 8.3 cm². Each reservoir was filled with 1 M VO²⁺ in 2 M H₂SO₄ solution (left side with 60 mL) and 1 M MgSO₄ in 2 M H₂SO₄ solution (right side with 60 mL), respectively. The solutions in both reservoirs were continuously stirred to avoid concentration polarization, while the concentration of VO²⁺ in the left chamber was measured by UV-Vis spectroscopy (VersaWave UV-Vis spectrometer) at 765 nm and room temperature. Aliquots of 50 µL were taken periodically from the left chamber and transferred to 950 µL MilliQ water to reach a 20-fold dilution factor in the cuvette. Finally, the vanadium ion permeability was calculated as:

$$P = \frac{V_R L}{A(C_L - C_R(t))} \frac{dC_R(t)}{dt} \quad (3)$$

where, *V_R* is volume of the reservoir; *L* is the thickness of the membrane; *A* is the active area of the membrane; *C_L* is the concentration of VO²⁺ in the left reservoir; and *C_R(t)* is the concentration of vanadium ion at time *t*.

2.5.4. Chemical stability of membranes

The chemical stability of the different membranes was evaluated by immersing small pieces of membranes in 10 mL of 1.6 M VO²⁺ in 2 M H₂SO₄ solution at room temperature for more than 400 h. To investigate any structural changes in the polymers, ¹H NMR spectra of immersed and pristine membranes were compared.

2.5.5. VRFB single-cell performance

VRFB single cells were assembled by placing the membranes between two carbon papers on each side, previously pre-treated with an effective area of 5 cm² and 0.22 mm of thickness. The electrodes were pre-treated at 500 °C for 3 h under the air atmosphere, and the membrane samples were immersed in 2 M H₂SO₄ solution for 24 h prior to measurements. The electrochemical cell (Fuel Cell Technologies) was provided with two Poco graphite plates with a serpentine flow field along with two Viton gaskets with a thickness of 1 mm for sealing. For flow battery measurements, volumes of 13 mL vanadium electrolyte solution (V^{3.5+} in 2 M H₂SO₄) were used on both sides of the cell with a circulation flow rate of 20 mL min⁻¹ using a dual-channel peristaltic pump (BT600L, Zhengzhou Mingyi Instrument Equipment Co., Ltd). The anolyte was under continuous nitrogen flow and the cell was galvanostatically charged-discharged at 130 mA cm⁻² for 50 cycles at room temperature using an 8-channel battery test system CT2001A (Landt Instruments) in the four-wire configuration. To avoid damage to the electrodes, and to preserve the stability of the electrolyte, the upper and lower limit of cut-off voltages was set at 1.7 V and 0.8 V for charge and discharge, respectively.

The membrane characteristics was evaluated by means of VRFB performance considering the coulombic (CE), voltage (VE) and energy (EE) efficiency, respectively, calculated as:

$$CE(\%) = \frac{Q_d}{Q_c} \cdot 100\% \quad (4)$$

$$VE(\%) = \frac{V_{d,avg}}{V_{c,avg}} \cdot 100\% \quad (5)$$

$$EE(\%) = CE \cdot VE\% \quad (6)$$

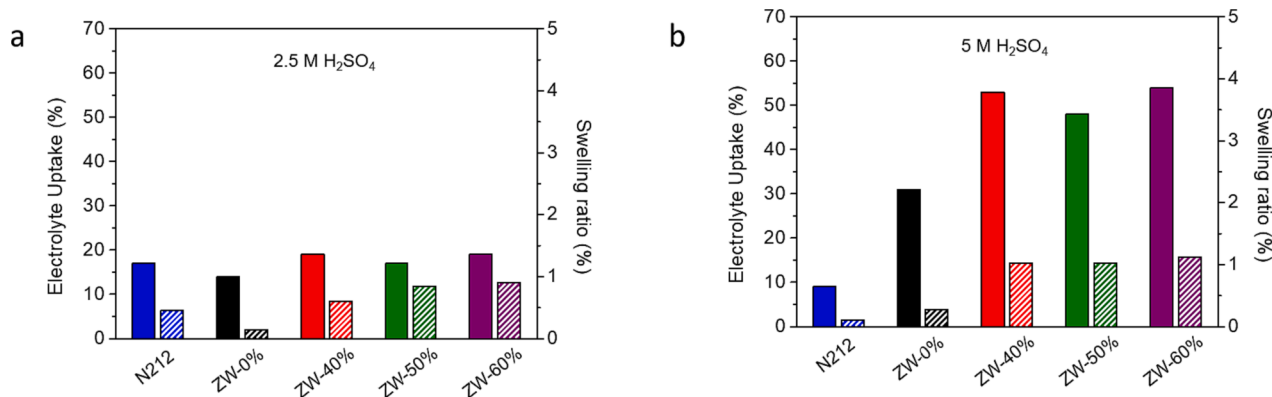


Fig. 2. Electrolyte uptake (filled columns) and swelling ratio (unfilled columns) of membranes after immersion in a) 2.5 M and b) 5.0 M H₂SO₄ solutions.

where Q_d and Q_c correspond to the capacity at the discharge and charge rate, respectively; and $V_{d,avg}$ and $V_{c,avg}$ correspond to the average voltage at discharge and charge state, respectively. Moreover, the rate performance was conducted at different current rates from 40 to 200 mA cm⁻² for 5 cycles per each.

For long-term test, galvanostatic cycling at 130 mA cm⁻² for 500 cycles were conducted on selected zwitterionic membranes at room temperature. During the galvanostatic cycling test, to check the membrane stability, the capacity retention and capacity loss were obtained as:

$$\text{Capacity retention}(\%) = \frac{Q_{d,n}}{Q_{d,1}} \hat{A} \cdot 100\% \quad (7)$$

$$\text{Capacity loss}(Q_{\text{loss}}\%) = \frac{Q_{th} - Q_{d,n}}{Q_{th} \hat{A} \cdot \text{cycle}} \hat{A} \cdot 100\% \quad (8)$$

where $Q_{d,n}$, $Q_{d,1}$ and Q_{th} correspond to the capacity at the discharge rate at n -th cycle, the discharge at first cycle, and the theoretical capacity, respectively.

Electrochemical Impedance Spectroscopy (EIS) was employed to measure the resistivity of the membranes using a four-probe VersaSTAT 4 workstation in a frequency range of 10⁶ Hz–10 Hz with an amplitude perturbation wave of 5 mV. The membranes were soaked in 2 M H₂SO₄ solution for 24 h before assembling the membrane in the flow cell set-up (Fuel Cell Technologies (FCT)). The measurements were conducted at room temperature and the high-frequency resistance of the membranes was obtained from the difference of R_w and R_{wo} (resistances with and without membrane, respectively). Area Specific Resistance (ASR) was calculated by using the following equation:

$$\text{ASR} = (R_w - R_{wo})A \quad (9)$$

where, A is the membrane cross-sectional active area (5 cm²).

Furthermore, the total resistance (R) of the cell was measured for both N212 and the zwitterionic membranes by placing the samples into the flow cell containing the vanadium electrolyte at a continuous flow rate of 20 mL min⁻¹. First, the cell was charged at 50 % of SoC and then polarized at different current rates, from 2 to 160 mA cm⁻², while the average cell potential was simultaneously recorded for 1 min. The measurements were conducted at room temperature, and R can be determined according to Ohm's law.

Lastly, the self-discharge duration of the VRFB was evaluated by galvanostatically charging the system to reach a 100 % State of Charge (SoC) and then keeping the system at open circuit voltage (OCV) over time.

3. Results and discussion

3.1. Monomer and polymer synthesis and characterization

In previous studies on amphoteric poly(arylene alkylene)s [32,33], the zwitterionic groups have been introduced to the polymer structure by post-polymerization modifications. In the present work a zwitterionic monomer, zwPip, was first synthesized and then used together with *p*-terphenyl and Pip in co-polyhydroxyalkylation reactions [34]. The zwPip monomer was obtained by quaternization of Pip in a sulfoalkylation reaction with 1,4-butane sultone. ¹H NMR analysis confirmed the structure, which was mainly in the gem diol form since the spectrum was recorded in D₂O. As seen in Fig. 1a, the signals originating from the hydrogens of the methylene units in the ring were found at 2 ppm and 3.4 ppm, and a triple signal at 2.9 ppm was attributed to the methylene groups closest to the sulfonate group. By adjusting the feeding ratio between the two ketones, zwPip and Pip, three copolymers, i.e., ZW-40, -50, and -60%, were synthesized with a controlled zwitterionic content (Fig. 1).

In order to achieve the desired structure of the copolymers, a 20% excess of Pip in relation to zwPip was used due to the higher reactivity of latter ketone. The structure and composition of the copolymers obtained by ¹H NMR spectroscopy analysis showed that the signals in the aromatic region, i. e., 7–8 ppm, arose from the hydrogens of the *p*-terphenyl moieties, while the hydrogens of the methyl and methylene groups of the piperidine rings and the pendant sulfoalkyl units showed up at 1.5 to 3.6 ppm. TFA (3–6 vol%) was added to all ¹H NMR samples in order to shift the water signal downfield and to protonate any tertiary amine groups, which then showed a signal above 9 ppm. Comparing the integral of the signals in the aromatic region with that of the protonated tertiary amines confirmed the successful synthesis and the control of the zwitterionic content in the copolymers.

3.2. Ex situ and in-situ characterization of zwitterionic (ZW) membranes

3.2.1. Electrolyte uptake and swelling ratio

The electrolyte uptake and the swelling ratio are important parameters since they significantly influence the performance of the ion exchange membranes. Excessive values of EU and SR may lead to mechanical failure and ion selectivity issues. The uptake of electrolyte and swelling values were evaluated in two different equilibrating solutions (2.5 M and 5 M H₂SO₄) for all membranes. According to the data in Fig. 2a, the electrolyte uptake in 2.5 M acid was around 20% for all the zwitterionic membranes, which was similar to N212. The swelling increased with increasing SW content. In the stronger acid (5 M H₂SO₄) the electrolyte uptake more than doubled for the zwitterionic membranes in comparison to the N212 membrane, that has a lower uptake and swelling in the stronger acid. The in- and through-plane data can be

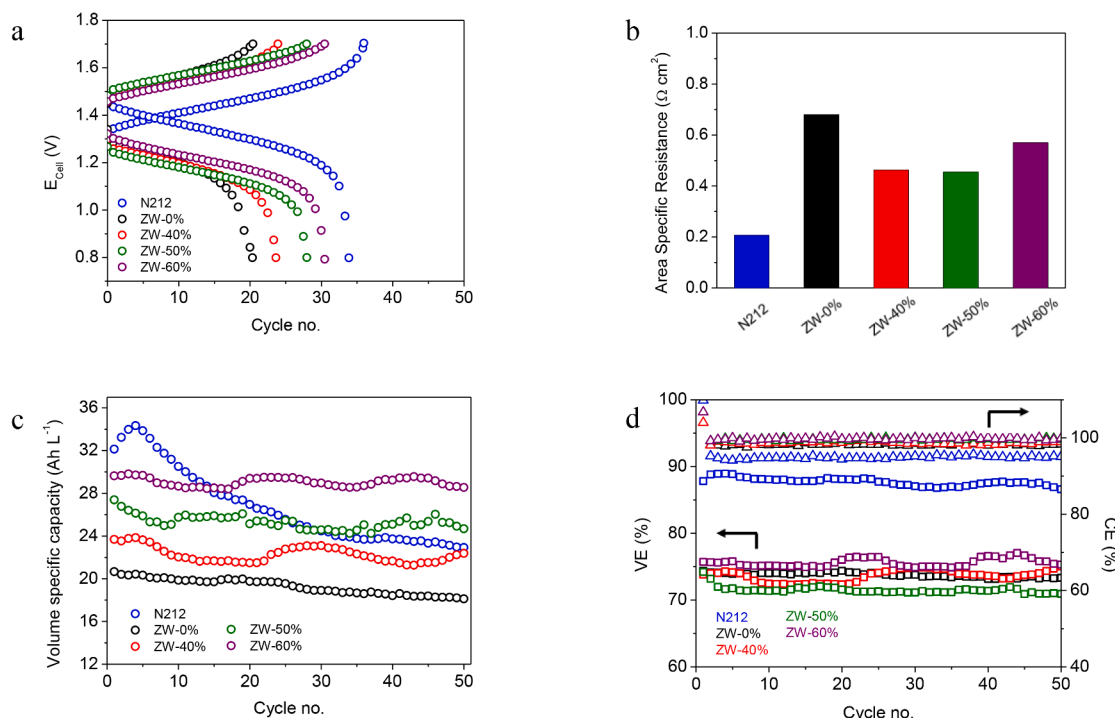


Fig. 3. VRFB cycling performance based on N212 and zwitterionic membranes as ion exchange membranes; (a) 5th cycle of the VRFB system; (b) ASR of different membranes using 2 M H_2SO_4 electrolyte; (c) discharge capacity over 50 cycles at a constant current of 130 mA cm^{-2} and (d) coulombic and voltage efficiencies over 50 cycles at a constant current of 130 mA cm^{-2} ; Experimental conditions: 1.6 M V^{3+} as negative electrolyte and 1.6 M VO^{2+} as positive electrolyte (both in 2 M H_2SO_4 as supporting electrolyte) 40 mL min^{-1} as flow rate and temperature of 24°C .

found in Table S1. The larger uptake at the higher acid concentration was most probably due to an increase in the degree of protonation of the piperidine rings, which increased the total ionic content of the copolymers and to a higher absorbance of sulfate ions and protons [35]. The decreasing electrolyte uptake and swelling ratio with increasing the acidic concentration for N212 is in agreement with a study by Hensensmeier et al., where the main reason for this phenomenon was stated to be the osmotic pressure [36].

The high electrolyte uptake, reaching up to 30–50%, for the zwitterionic membranes in 5 M H_2SO_4 , was too high to ensure reliable mechanical integrity. However, the values reached by the membranes in the 2.5 M H_2SO_4 solution are moderate, indicating that this concentration range is more suitable for proper membrane performance. Hence, in this study, a commercial vanadium electrolyte solution containing 2 M H_2SO_4 was used to evaluate the single-cell performance.

3.2.2. VRFB performance

The electrochemical performance of a single-cell VRFB using N212 and synthesized ZW membranes with different contents of zwitterionic groups was investigated. Charge-discharge cycles were conducted at a current density of 130 mA cm^{-2} . Fig. 3a shows the charge-discharge curves of the VRFB at the 5th cycle. All curves show Nernstian behavior and follow a trend of increasing capacity with increasing zwitterionic content. The large polarisation observed for the zwitterionic membranes was associated to the relatively high Area Specific Resistance (ASR) values of membranes (Fig. 3b). The ASR of all membranes was measured using EIS prior to the cycling tests. Generally, the high-frequency resistance of the EIS corresponds to the total ionic and electronic resistance in the cell components like the membrane, electrolyte, electrode, and electronic contacts. Nevertheless, due to the high conductivity of electrolytes and electrodes, it is safe to assume that only the membrane resistance significantly contributed to the high-frequency resistance. As shown in Fig. 3b, membranes with the same thickness (ca. $50 \mu\text{m}$) show that the N212 perfluorinated membrane (used as a benchmark) provides

Table 1

Total resistance of the VRFB obtained from the polarization curves before and after the galvanostatic cycling tests.

Membranes	Zwitterionic content% (Pip and SO_3)	Piperidinium content%	VRFB resistance before cycling ($\Omega \text{ cm}^2$)	VRFB resistance after cycling ($\Omega \text{ cm}^2$)
N212	only SO_3	n/a	0.69	0.85
ZW-0	0	100	1.57	1.77
ZW-40	40	60	1.81	2.10
ZW-50	50	50	1.68	2.05
ZW-60	60	40	1.45	1.57

high ion conductivity in acidic media due to the densely and highly acidic sulfonic acid groups attached to the main polymer chains. Thus, it is reasonable to expect higher ASR values for the ZW membranes than for N212. Generally, the area-specific resistance was suppressed by a factor of 1.2–1.5 when incorporating the zwitterionic groups in the polymer backbone. Evidently, the increasing capacity with SW content do not follow the ASR trend. In addition to ASR measurement with EIS, polarisation and so, resistance was also extracted from polarisation curves (see Fig. S1) the measured values before and after cycling are found in Table 1. From these resistances, it is clear that the resistance of the cell decreases with increasing SW content and thus follows the trend for polarization and capacity in Fig. 2 a and c.

The corresponding cell capacities and coulombic efficiencies (CE) over time are shown in Fig. 3c and 3d. As seen, the commercial N212 membrane showed a large capacity decay that sharply decreased in the first 20–25 cycles, which can be attributed to the different levels of crossover of vanadium species [37–39]. Generally, the crossover influences the distribution of the vanadium species and water molecules between the half-cells, resulting in an unbalanced amount and composition of the electrolytes. In contrast, the discharge capacity of the

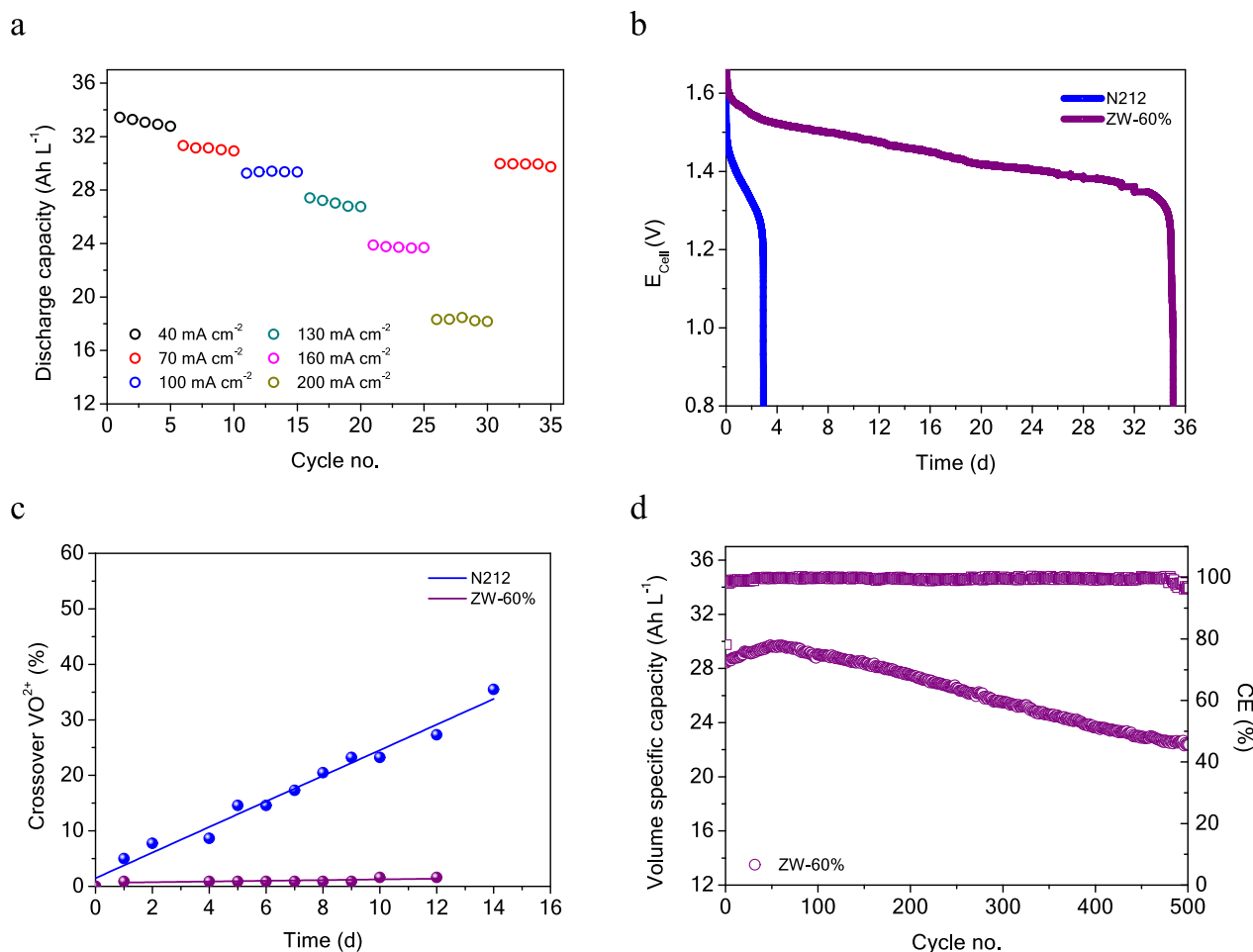


Fig. 4. VRFB cycling performance zwitterionic membrane (ZW-60%) as ion exchange membranes; (a) rate performance; (b) self-discharge duration in open circuit condition; (c) crossover data of vanadium(IV) through the N212 and ZW-60% membranes as a function of time; (d) long-term cycling performance with the ZW-60% membrane over 500 cycles at constant current of 130 mA cm⁻²; Experimental conditions 1.6 M V³⁺ as negative electrolyte and 1.6 M VO²⁺ as positive electrolyte (both in 2 M H₂SO₄ as supporting electrolyte) 40 mL min⁻¹ as flow rate and temperature of 24 °C.

zwitterionic membranes remained relatively stable over the first 50 cycles. It is interesting and instructive to consider the open circuit voltage (OCV) of the VRFB directly after the charge and discharge processes and correlate it to capacity loss. As seen in Fig. S2, the OCV of the VRFB using N212 exhibits a decreasing and increasing rate during 50 cycles after charge and discharge, respectively, meaning that the electrolyte crossover cases a mixed potential and a gradual voltage loss at constant current density, which is translated to capacity loss. Despite N212, stable OCV was observed for VRFB using ZW-60%. Further, the capacity was critically dependent on the ZW content, 50% higher capacity was achieved for ZW-60%. Interestingly, the capacity loss (see Fig. S3) has been significantly reduced using ZW-40%, -50% and -60% (ranging from 1.14 to 1.33 %Q_{loss}/cycle in 50 cycles) compared to the ZW-0% (1.46 %Q_{loss}/cycle in 50 cycles) carrying only piperidinium groups [28]. This means that the combination of zwitterionic and piperidinium groups was beneficial in controlling the electrolyte crossover.

Comparing the efficiencies in Fig. 3d, the VRFBs containing zwitterionic membranes showed CE over 97%, which was higher than the system based on N212 (approx. 95%). The voltage efficiency were relatively similar around 75% for the synthesized membranes. It should be noted that the relatively low voltage efficiency is mainly due to the high current density at which the VRFB was operated.

The total resistance of the VRFB and the resulting polarization curves were acquired at 50% SoC under the same experimental conditions and are given in Table 1 and Fig. S1. The synthesized membranes initially

showed more than twice the resistivity of N212, which is in accordance with the data in Fig. 3b. Among the synthesized membranes, the total resistance is relatively low for the membrane without the ZW group before cycling but increases by adding 40% ZW groups. By further adding ZW groups (40% to 60%), the total resistance shows a reduction rate (from 1.8 to 1.45).

It should be mentioned that the total resistance values do not follow the ASR trend observed in Fig. 3b. This is likely due to the different experimental conditions that were used for measuring ASR and total resistances generating different mechanisms. After the VRFB tests, the total resistance increased using all membranes; the most significant rise corresponds to the VRFB using N212 with 23%, and the slightest increase was for ZW-60% from 1.45 to 1.57 Ω cm² corresponds to only 8%, which shows the well electrochemical performance of the membrane.

Moreover, taking into account the different degrees of functionality of these novel membranes, the total resistance both before and after cycling showed greater performance with increasing zwitterionic content, with the exception of the non-quaternised membrane (ZW-0%). One may expect the lowest performance when using the ZW-0% membrane. However, the obtained ASR is not as high as expected. This may partly be due to the microstructural effects of entangling polymer chains and the phase separation in the membrane. Still, a clear tendency was observed with the zwitterionic content when comparing the electrochemical cell performances.

The enhanced capacity demonstrated when incorporating a larger content of the zwitterionic groups in the membranes (see Fig. 3c) may be

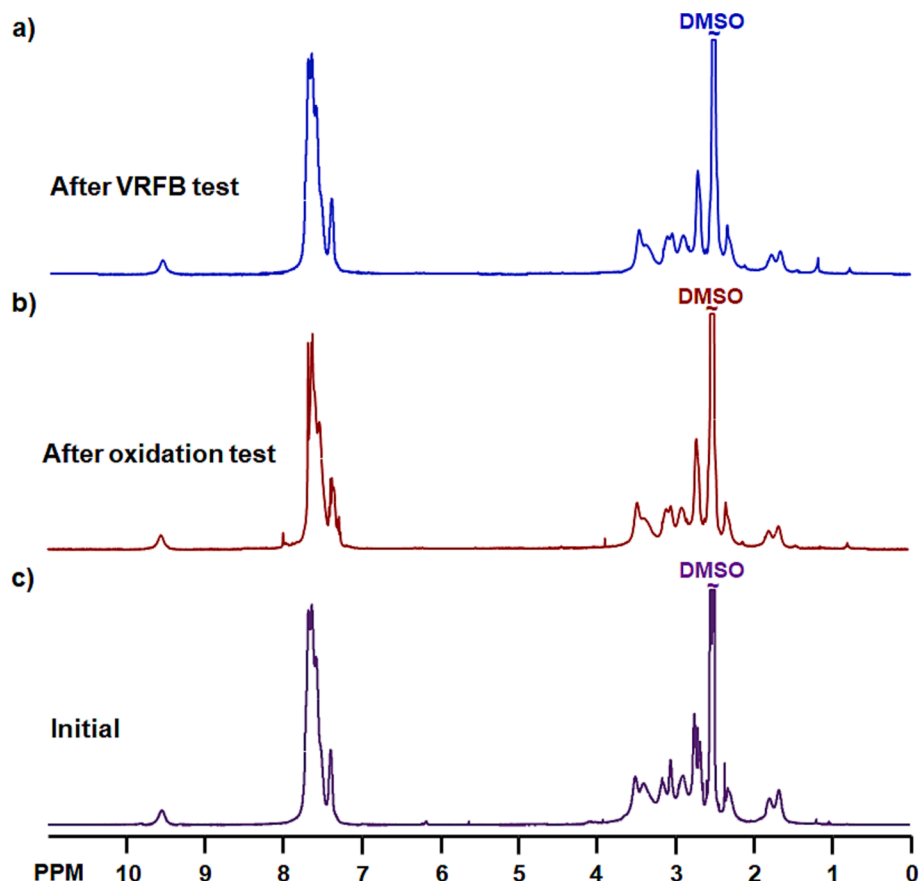


Fig. 5. ^1H NMR spectra of ZW-60%: (a) initial sample, (b) after the exposure to the oxidative solution, and (c) after VRFB test.

explained by the fact that the proton mobility is more pronounced compared to the (bi)sulfate ions mobility [40] since there is an increase in negatively charged sulfonic acid groups in the polymer structure in comparison to the positively charged piperidinium groups. In addition, since the overall net charge of the polymer remains positive, the Donnan exclusion effect is still preserved. The enhanced selectivity for protons is suggested to provide excellent capacity stability over time and low crossover VO^{2+} rates. Consequently, the membranes with low zwitterionic content showed lower battery performance, and this is mainly attributed to the conductivity of membranes, which follows from the ASR values obtained for each membrane. Attempts were made to increase the zwitterionic content of the membranes further. However, this was not possible because of severe limitations in the solubility of these copolymers during the synthesis. The best battery performance in this study was thus obtained by membrane ZW-60% with the highest zwitterionic content, and the tendency observed in this family of membranes was: ZW-60% > ZW-50% > ZW-40% > ZW-0%, as illustrated in Fig. 3d. It should be noted that the lower discharge capacity observed with ZW-0%, as compared to N212, was likely due to the absence of zwitterionic groups or, more precisely, the absence of sulfonic acid groups.

Following these results, the rate performance of a VRFB with the ZW-60% membrane was investigated for varying current densities. As shown in Fig. 4a, the rate performance of the VRFB exhibited a low cell overpotential by increasing the current density (from 40 to 200 mA cm^{-2}) and returning to 70 mA cm^{-2} . The self-discharge investigation was of interest to foresee the capability of the membrane in stabilizing the OCV, which is a major deciding factor for the VRFB lifetime. Hence, the single cell was charged to 100% SoC at a slow current rate and then kept idle. The self-discharge duration of VRFBs with ZW-60% and N212 was evaluated for comparison (Fig. 4b). The self-discharge using N212 was 67 h (around three days) for the consumption of V^{2+} and VO_2^+

electrolytes, which agrees with the previous studies [41]. However, with ZW-60%, the self-discharge remarkably took over 840 h (35 days). The results of this comparison emphasize that the ZW-60% membrane has a superior suppression of electrolyte crossover compared to most membranes, particularly N212. Notably, the OCV performance of ZW-60% was significantly higher than that of other alternative membranes reported in the literature [30,42–46]. This further confirms the excellent ion selectivity of the membrane and, consequently, the low capacity losses due to vanadium crossover. To support the latter, the vanadium ion permeability, which is one of the most important features required of membranes for the long-term operation of VRFB, was measured. Systems with high vanadium permeation rates may suffer from battery self-discharge and progressive capacity decay. Consequently, it is of crucial importance to design and employ a membrane capable of reducing the cross-mixing of active species while preserving a high ion conductivity. In the present case, as depicted in Fig. 4c, the data showed a substantial permeation of vanadium(IV) ions through N212. After 12 h, 30% of the VO^{2+} had permeated over to the MgSO_4 side. In comparison, the ZW-60% membrane was, in principle, impermeable for VO^{2+} , and only about 1% was found in the solution after the same period. The high capability retention using ZW-60% was observed in the long-term cycling of the VRFB (500 cycles of charge/discharge) at 130 mA cm^{-2} and is displayed in Fig. 4d. Even though a slight loss is observed after the first 60 cycles, the membrane maintained stable operation, reaching 78.7% of capacity retention after 500 cycles. It should be noted that N212 showed a similar loss already after 25 cycles. These results demonstrate the outstanding properties of the zwitterionic membranes, which qualify them as potential candidates for practical applications in VRFBs.

The VRFB tests also provide excellent indications of the in-situ mechanical stability of the membranes [26]. Mechanical strength is essential for membranes' performance and can be measured through ex-

situ tensile tests or in-situ flow cell methods. In this context, a typical ex-situ test does not necessarily reflect the mechanical stability of the membranes in the flow cell. Similar to ASR measurements (Table 1), evaluating the mechanical strength of membranes in the flow cell is more relevant since it is measured under more realistic conditions with a combination of tensile and compressive forces. In the present case, the membranes remained stable with no damage or cracks under standard conditions for 500 cycles. Hence, the membranes were considered mechanically stable in the current application.

Last but not least, membrane oxidation stability is an inherent property of crucial importance to extend the lifetime of the battery. Here, the stability was evaluated by immersing the membranes in 1.6 M VO_2^+ in 2 M aqueous H_2SO_4 solution at room temperature for over 400 h. The ^1H NMR spectra after the exposure to the oxidative solution showed no specific changes compared to those of pristine samples, which verified that the main backbone of the polymer and the ionic moieties had high stability under the investigated conditions (Fig. 5 and Fig. S4). Similar ^1H NMR results were achieved after 500 cycles with no change in the molecular structure compared to the pristine samples. These results are in agreement with the reported results on poly(arylene piperidinium) membranes, which also showed very high oxidation stability [41]. Overall, these membranes demonstrate excellent chemical stability after battery operation.

4. Conclusion

A series of poly(terphenylene)-based membranes containing zwitterionic (sulfoalkylated piperidinium) and cationic piperidinium groups in different ratios were synthesized and evaluated for VRFB application. The zwitterionic content was controlled in copolymerizations involving mixtures with specific nonionic and zwitterionic monomers ratios. Although the conductivity of these membranes was lower than that of N212, the zwitterionic groups suppressed the ohmic resistivity of the membranes by a factor of up to 1.5 compared to the corresponding non-zwitterionic form due to the incorporation of the pendant sulfonic acid groups. The VRFB single-cell study using zwitterionic membranes showed a stable discharge capacity with almost no capacity loss for over 50 cycles. Among the synthesized membranes, the VRFB operating with the membrane containing 60% zwitterionic groups showed the best performance, including a superior discharge capacity and efficiency. Accordingly, outstanding self-discharge durability (greater than 800 h) and excellent rate performance were achieved for the VRFB using ZW-60%. More important, the ZW-60% membrane demonstrated long-term cycling tests (500 cycles) with an average CE of 96.5% at 130 mA cm^{-2} and capacity retention of approximately 79%. The ^1H NMR data subsequently proved that the ZW-60% had excellent (electro)chemical stability.

Declaration of Competing Interest

The authors declare that they have no known competing financial interests or personal relationships that could have appeared to influence the work reported in this paper.

Data availability

Data will be made available on request.

Acknowledgements

This work has been funded by the Swedish Energy Agency (project number P2021-90002) and the European Union under the HIGREEW project, Affordable High-performance Green Redox Flow batteries (Grant agreement no. 875613). H2020: LC-BAT-4-2019.

Appendix A. Supplementary data

Supplementary data to this article can be found online at <https://doi.org/10.1016/j.cej.2023.145879>.

References

- [1] B. Dunn, H. Kamath, J.-M. Tarascon, Electrical energy storage for the grid: a battery of choices system, *Science* 334 (2011) 928–935, <https://doi.org/10.1126/science.1212741>.
- [2] C. Zhang, L. Zhang, Y. Ding, S. Peng, X. Guo, Y. Zhao, G. He, G. Yu, Progress and prospects of next-generation redox flow batteries, *Energy Storage Mater.* 15 (2018) 324–350, <https://doi.org/10.1016/j.ensm.2018.06.008>.
- [3] A. Poullikkas, A comparative overview of large-scale battery systems for electricity storage, *Renew. Sustain. Energy Rev.* 27 (2013) 778–788, <https://doi.org/10.1016/j.rser.2013.07.017>.
- [4] A.Z. Weber, M.M. Mench, J.P. Meyers, P.N. Ross, J.T. Gostick, Q. Liu, Redox flow batteries: a review, *J. Appl. Electrochem.* 41 (2011) 1137–1164, <https://doi.org/10.1007/s10800-011-0348-2>.
- [5] J. Cho, S. Jeong, Y. Kim, Commercial and research battery technologies for electrical energy storage applications, *Prog. Energy Combust. Sci.* 48 (2015) 84–101, <https://doi.org/10.1016/j.pecs.2015.01.002>.
- [6] J. Ye, L. Xia, C. Wu, M. Ding, C. Jia, Q. Wang, Redox targeting-based flow batteries, *J. Phys. D Appl. Phys.* 52 (2019) 443001–443018, <https://doi.org/10.1088/1361-6463/ab3251>.
- [7] A. Parasuraman, T.M. Lim, C. Menictas, M. Skyllas-Kazacos, Review of material research and development for vanadium redox flow battery applications, *Electrochim. Acta* 101 (2013) 27–40, <https://doi.org/10.1016/j.electacta.2012.09.067>.
- [8] G. Kear, A.A. Shah, F.C. Walsh, Development of the all-vanadium redox flow battery for energy storage: a review of technological, financial and policy aspects, *Int. J. Energy Res.* 36 (2012) 1105–1120, <https://doi.org/10.1002/er.1863>.
- [9] K. Lourenssen, J. Williams, F. Ahmadpour, R. Clemmer, S. Tasnim, Vanadium redox flow batteries: a comprehensive review, *J. Energy Storage*. 25 (2019) 100844–100861, <https://doi.org/10.1016/j.est.2019.100844>.
- [10] R.A. Elgammal, Z. Tang, C.N. Sun, J. Lawton, T.A. Zawodzinski, Species uptake and mass transport in membranes for vanadium redox flow batteries, *Electrochim. Acta* 237 (2017) 1–11, <https://doi.org/10.1016/j.electacta.2017.03.131>.
- [11] N. Poli, M. Schäffer, A. Trovò, J. Noack, M. Guarneri, P. Fischer, Novel electrolyte rebalancing method for vanadium redox flow batteries, *Chem. Eng. J.* 405 (2021) 126583–126596, <https://doi.org/10.1016/j.cej.2020.126583>.
- [12] T. Jirabovornwisut, A. Arpornwichanop, A review on the electrolyte imbalance in vanadium redox flow batteries, *Int. J. Hydrogen Energy* 44 (2019) 24485–24509, <https://doi.org/10.1016/j.ijhydene.2019.07.106>.
- [13] K.E. Rodby, T.J. Carney, Y. Ashraf Gandomi, J.L. Barton, R.M. Darling, F. R. Brushett, Assessing the leveled cost of vanadium redox flow batteries with capacity fade and rebalancing, *J. Power Sources* 460 (2020) 227958–227969, <https://doi.org/10.1016/j.jpowsour.2020.227958>.
- [14] C. Minke, T. Turek, Economics of vanadium redox flow battery membranes, *J. Power Sources* 286 (2015) 247–257, <https://doi.org/10.1016/j.jpowsour.2015.03.144>.
- [15] M. Zhang, M. Moore, J.S. Watson, T.A. Zawodzinski, R.M. Counce, Capital cost sensitivity analysis of an all-vanadium redox-flow battery, *J. Electrochem. Soc.* 159 (2012) A1183–A1188, <https://doi.org/10.1149/2.041208jes>.
- [16] X. Teng, J. Dai, J. Su, Y. Zhu, H. Liu, Z. Song, A high performance polytetrafluoroethylene/naion composite membrane for vanadium redox flow battery application, *J. Power Sources* 240 (2013) 131–139, <https://doi.org/10.1016/j.jpowsour.2013.03.177>.
- [17] X. Teng, C. Sun, J. Dai, H. Liu, J. Su, F. Li, Solution casting naion/polytetrafluoroethylene membrane for vanadium redox flow battery application, *Electrochim. Acta* 88 (2013) 725–734, <https://doi.org/10.1016/j.electacta.2012.10.093>.
- [18] K.J. Lee, Y.H. Chu, Preparation of the graphene oxide (GO)/naion composite membrane for the vanadium redox flow battery (VRB) system, *Vacuum* 107 (2014) 269–276, <https://doi.org/10.1016/j.vacuum.2014.02.023>.
- [19] J. Kim, J.D. Jeon, S.Y. Kwak, Naion-based composite membrane with a permselective layered silicate layer for vanadium redox flow battery, *Electrochem. Commun.* 38 (2014) 68–70, <https://doi.org/10.1016/j.elecom.2013.11.002>.
- [20] J. Xi, Z. Wu, X. Qiu, L. Chen, Naion/SiO₂ hybrid membrane for vanadium redox flow battery, *J. Power Sources* 166 (2007) 531–536, <https://doi.org/10.1016/j.jpowsour.2007.01.069>.
- [21] J. Ye, X. Zhao, Y. Ma, J. Su, C. Xiang, K. Zhao, M. Ding, C. Jia, L. Sun, Hybrid membranes dispersed with superhydrophilic TiO₂ nanotubes toward ultra-stable and high-performance vanadium redox flow batteries, *Adv. Energy Mater.* 10 (2020) 1904041–1904048, <https://doi.org/10.1002/aenm.201904041>.
- [22] T.N.L. Doan, T.K.A. Hoang, P. Chen, Recent development of polymer membranes as separators for all-vanadium redox flow batteries, *RSC Adv.* 5 (2015) 72805–72815, <https://doi.org/10.1039/c5ra05914c>.
- [23] S. Maurya, S.H. Shin, Y. Kim, S.H. Moon, A review on recent developments of anion exchange membranes for fuel cells and redox flow batteries, *RSC Adv.* 5 (2015) 37206–37230, <https://doi.org/10.1039/c5ra04741b>.
- [24] L. Zeng, T.S. Zhao, L. Wei, H.R. Jiang, M.C. Wu, Anion exchange membranes for aqueous acid-based redox flow batteries: Current status and challenges, *Appl.*

- Energy 233–234 (2019) 622–643, <https://doi.org/10.1016/j.apenergy.2018.10.063>.
- [25] Z. Yuan, X. Li, Y. Zhao, H. Zhang, Mechanism of polysulfone-based anion exchange membranes degradation in vanadium flow battery, *ACS Appl. Mater. Interfaces* 7 (2015) 19446–19454, <https://doi.org/10.1021/acsami.5b05840>.
- [26] A. Khataee, H. Nederstedt, P. Jannasch, R.W. Lindström, Poly(arylene alkylene)s functionalized with perfluorosulfonic acid groups as proton exchange membranes for vanadium redox flow batteries, *J. Membr. Sci.* 671 (2023) 121390–121401, <https://doi.org/10.1016/j.memsci.2023.121390>.
- [27] T. Wang, J.Y. Jeon, J. Han, J.H. Kim, C. Bae, S. Kim, Poly(terphenylene) anion exchange membranes with high conductivity and low vanadium permeability for vanadium redox flow batteries (VRFBs), *J. Membr. Sci.* 598 (2020) 117665–117672, <https://doi.org/10.1016/j.memsci.2019.117665>.
- [28] J. Skvaril, A. Avelin, J. Sandberg, E. Dahlquist, The experimental study of full-scale biomass-fired bubbling fluidized bed boiler, *Energy Procedia* (2014) 643–647, <https://doi.org/10.1016/j.egypro.2014.11.1188>.
- [29] C.H. Lin, M.C. Yang, H.J. Wei, Amino-silica modified nafion membrane for vanadium redox flow battery, *J. Power Sources* 282 (2015) 562–571, <https://doi.org/10.1016/j.jpowsour.2015.02.102>.
- [30] S. Liu, L. Wang, D. Li, B. Liu, J. Wang, Y. Song, Novel amphoteric ion exchange membranes by blending sulfonated poly(ether ether ketone)/quaternized poly(ether imide) for vanadium redox flow battery applications, *J. Mater. Chem A Mater.* 3 (2015) 17590–17597, <https://doi.org/10.1039/c5ta04351d>.
- [31] X. Yan, C. Zhang, Y. Dai, W. Zheng, X. Ruan, G. He, A novel imidazolium-based amphoteric membrane for high-performance vanadium redox flow battery, *J. Membr. Sci.* 544 (2017) 98–107, <https://doi.org/10.1016/j.memsci.2017.09.025>.
- [32] X. Yan, H. Zhang, Z. Hu, L. Li, L. Hu, Z. Li, L. Gao, Y. Dai, X. Jian, G. He, Amphoteric-side-chain-functionalized “ether-free” poly(arylene piperidinium) membrane for advanced redox flow battery, *ACS Appl. Mater. Interfaces* 11 (2019) 44315–44324, <https://doi.org/10.1021/acsami.9b15872>.
- [33] H. Zhang, Z. Li, L. Hu, L. Gao, M. Di, Y. Du, X. Yan, Y. Dai, X. Ruan, G. He, Covalent/ionic co-crosslinking constructing ultra-densely functionalized ether-free poly(biphenylene piperidinium) amphoteric membranes for vanadium redox flow batteries, *Electrochim. Acta* 359 (2020) 136879–136905, <https://doi.org/10.1016/j.electacta.2020.136879>.
- [34] A. Shirole, P.M. Bakvand, P. Jannasch, Hydroxide ion conducting membranes dually functionalized with cationic and zwitterionic groups, *ACS Appl. Energy Mater.* 6 (13) (2023) 7240–7249.
- [35] M. Jung, W. Lee, C. Noh, A. Kononova, G.S. Yi, S. Kim, Y. Kwon, D. Henkensmeier, Blending polybenzimidazole with an anion exchange polymer increases the efficiency of vanadium redox flow batteries, *J. Membr. Sci.* 580 (2019) 110–116, <https://doi.org/10.1016/j.memsci.2019.03.014>.
- [36] Y. Lee, S. Kim, R. Hempelmann, J.H. Jang, H.J. Kim, J. Han, J. Kim, D. Henkensmeier, Nafion membranes with a sulfonated organic additive for the use in vanadium redox flow batteries, *J. Appl. Polym. Sci.* 136 (2019) 47547–47557, <https://doi.org/10.1002/app.47547>.
- [37] A. Tang, J. Bao, M. Skyllas-Kazacos, Dynamic modelling of the effects of ion diffusion and side reactions on the capacity loss for vanadium redox flow battery, *J. Power Sources* 196 (2011) 10737–10747, <https://doi.org/10.1016/j.jpowsour.2011.09.003>.
- [38] C. Sun, J. Chen, H. Zhang, X. Han, Q. Luo, Investigations on transfer of water and vanadium ions across Nafion membrane in an operating vanadium redox flow battery, *J. Power Sources* 195 (2010) 890–897, <https://doi.org/10.1016/j.jpowsour.2009.08.041>.
- [39] Q. Luo, L. Li, W. Wang, Z. Nie, X. Wei, B. Li, B. Chen, Z. Yang, V. Sprenkle, Capacity decay and remediation of nafion-based all-vanadium redox flow batteries, *ChemSusChem* 6 (2013) 268–274, <https://doi.org/10.1002/cssc.201200730>.
- [40] P.W. (Peter W. Atkins, Julio. De Paula, Physical chemistry for the life sciences, Oxford University Press (2006) ISBN: 0-7167-8759-8.
- [41] A. Khataee, D. Pan, J.S. Olsson, P. Jannasch, R.W. Lindström, Asymmetric cycling of vanadium redox flow batteries with a poly(arylene piperidinium)-based anion exchange membrane, *J. Power Sources* 483 (2021) 229202–229210, <https://doi.org/10.1016/j.jpowsour.2020.229202>.
- [42] J. Xu, S. Dong, P. Li, W. Li, F. Tian, J. Wang, Q. Cheng, Z. Yue, H. Yang, Novel ether-free sulfonated poly(biphenyl) tethered with tertiary amine groups as highly stable amphoteric ionic exchange membranes for vanadium redox flow battery, *Chem. Eng. J.* 424 (2021) 130314–130327, <https://doi.org/10.1016/j.cej.2021.130314>.
- [43] L. Zeng, T.S. Zhao, L. Wei, Y.K. Zeng, Z.H. Zhang, Highly stable pyridinium-functionalized cross-linked anion exchange membranes for all vanadium redox flow batteries, *J. Power Sources* 331 (2016) 452–461, <https://doi.org/10.1016/j.jpowsour.2016.09.065>.
- [44] J. Chen, C. Hou, G. Wu, K. Wang, H. Mao, H. Dong, Research on self-discharge characteristics of a vanadium redox-flow battery system (2016) ISBN: 978-1-60595-376-2.
- [45] J. Qiu, M. Zhai, J. Chen, Y. Wang, J. Peng, L. Xu, J. Li, G. Wei, Performance of vanadium redox flow battery with a novel amphoteric ion exchange membrane synthesized by two-step grafting method, *J. Membr. Sci.* 342 (2009) 215–220, <https://doi.org/10.1016/j.memsci.2009.06.043>.
- [46] J. Yuan, C. Yu, J. Peng, Y. Wang, J. Ma, J. Qiu, J. Li, M. Zhai, Facile synthesis of amphoteric ion exchange membrane by radiation grafting of sodium styrene sulfonate and N, N-dimethylaminoethyl methacrylate for vanadium redox flow battery, *J. Polym. Sci. A Polym. Chem.* 51 (2013) 5194–5202, <https://doi.org/10.1002/pola.26949>.